2024 EC³
2024 European Conference on Computing in Construction
Chania, Crete, Greece
July 15-17, 2024

IDENTIFICATION OF COMPOSITE SENSOR FAULTS IN STRUCTURAL HEALTH MONITORING SYSTEMS USING LONG SHORT-TERM MEMORY NETWORKS

Thamer Al-Zuriqat, Heba Al-Nasser, Kosmas Dragos, Chillón Geck, and Kay Smarsly
Hamburg University of Technology, Hamburg, Germany

Abstract

Fault identification (FI) is an integral part of sensor fault diagnosis in structural health monitoring (SHM) systems. However, current FI approaches often overlook composite sensor faults, i.e. different sensor fault types occurring simultaneously within an individual sensor. As a result, actual fault occurrences in real-world SHM systems may be underestimated. This paper introduces an FI approach utilizing long short-term memory networks, addressing composite faults. The FI approach is validated using sensor data recorded by a real-world SHM system. The results demonstrate the capability of the FI approach to identify composite sensor faults, thus enhancing the reliability and accuracy of fault diagnosis.

Introduction

Structural health monitoring (SHM) is a non-destructive evaluation technique employing data recorded by sensors ("sensor data") to assess structural conditions (Law et al., 2014). SHM aims to improve safety and cost efficiency in structural maintenance through filling gaps of periodic visual inspections (Cawley, 2018). Hardware or software errors, exposure to harsh environmental conditions, degradation, and signal interferences may lead to malfunctions of sensors ("faulty sensors") in SHM systems (Zhang et al., 2018). Consequently, faulty sensors may compromise the outcomes of SHM systems (Steiner et al., 2019).

In SHM systems, sensor fault types include bias, drift, gain, precision degradation, complete failure (constant or with noise), and outliers (Kullaa et al., 2013). Fault diagnosis approaches for SHM systems have been proposed based on either physical or analytical redundancy (Frank, 1990). Physical redundancy entails installing additional, i.e. "redundant", sensors and detecting faults based on sensor data comparisons. However, the high cost, power consumption, and maintenance associated with physical redundancy have been the primary motivation for developing analytical redundancy approaches (Smarsly & Petryna, 2014). In general, analytical redundancy employs mathematical models to characterize a system, leveraging the inherent redundancy present in the sensor data (Al-Zuriqat et al., 2023). Fault diagnosis using analytical redundancy comprises four steps (Patton, 1990):

- Fault detection
- Fault isolation
- Fault identification
- Fault accommodation

In the fault detection step, residuals between sensor data and corresponding "virtual outputs", derived from mathematical models, are evaluated using threshold logic or hypothesis testing (Isermann & Balle, 1997). In case faults are detected, fault isolation involves determining the locations of the faulty sensors. To gain insights into the underlying causes of sensor faults and define strategies for compensating for errors induced by sensor faults, the type or nature of the faults are determined in the fault identification (FI) step. Finally, in the fault accommodation step, data recorded by the faulty sensor is reconstructed using virtual outputs of the mathematical models.

Existing fault diagnosis approaches have mainly focused on detecting, isolating, and accommodating sensor faults. Rao et al. (2007) has presented a concept, originally proposed by Kramer (1992), introducing a null-subspace-based approach for sensor fault detection and isolation, combined with autoassociative neural networks for fault accommodation. Smarsly & Law (2014) have proposed a decentralized fault detection and isolation approach in wireless SHM systems employing artificial neural networks. The approach has been extended from the time domain to the frequency domain and has also accounted for the presence of structural damage (Dragos & Smarsly, 2016). Al-Zuriqat et al. (2023) have introduced an adaptive sensor fault detection, isolation, and accommodation approach for SHM systems using feedforward artificial neural networks with backpropagation, considering single sensor faults occurring simultaneously in individual sensors. Liu et al. (2022) have used stacked gated recurrent unit neural networks to detect, isolate and accommodate sensor faults, and global-local logic to differentiate sensor faults from structural damage.

Among fault diagnosis approaches that include FI, Fritz et al. (2022) have proposed an analytical-redundancy approach, which integrates feedforward artificial neural networks and convolutional neural networks to detect, isolate, identify, and accommodate sensor faults. Additionally, other approaches, based on generalized likelihood ratio (Li et al., 2019), on generalized quasi-natural analogy test principle (Yan et al., 2020), and on set theory and support vector machine (Yu et al., 2014), have also addressed the FI step. However, in the aforementioned studies, only single sensor faults have been considered, i.e. one sensor fault type within each individual sensor. Moreover, not all sensor fault types have been addressed. For example, outliers (Fritz et al. 2022; Li et al., 2019), drift, precision degradation, and complete failure (Yan et al., 2020) have not been included.

Sensors in SHM systems may experience combinations of faults, i.e. faults of different types occurring simultaneously within an individual sensor (hereinafter termed "composite sensor faults"). The plausibility of

composite sensor faults occurrence in SHM systems has been corroborated in Li et al. (2022), in which composite sensor faults have been observed during experimentation, specifically gain and drift in one sensor.

In summary, despite the importance of FI in gaining insights into underlying causes of sensor faults within SHM systems, current FI approaches often fail to account for composite sensor faults, which may manifest in real-world SHM systems (Li et al., 2022). In this paper, an approach towards identification of composite sensor faults (ICSF) is proposed. Sensor data with artificially injected composite sensor faults is used to train long short-term memory (LSTM) classification networks, addressing composite sensor faults.

The remainder of the paper is organized as follows: First, composite sensor faults in SHM systems are elucidated. Then, a description of the ICSF approach is introduced. Next, the implementation and validation of the ICSF approach are presented, and the results are discussed. Finally, the paper ends with a summary and conclusions, and an outlook on future research is provided.

Composite sensor faults

Sensor fault types manifest into errors, which have distinct footprints on sensor data. For example, a bias is represented by a constant deviation of the sensor data from the values that should be measured ("actual values", e.g. structural responses or environmental parameters). A drift is characterized by the gradual deviation of sensor data from the actual values over time. A gain occurs when sensor data is systematically scaled by a constant value. Precision degradation is caused by the contamination of sensor data with noise. A complete failure is observed as sensor data consisting of a constant value ("complete failure constant") or noise ("complete failure with noise"), regardless of changes occurring in the actual values. Finally, an outlier manifests as a discontinuous observation in the sensor data that deviates from the actual values at isolated time instances.

The aforementioned sensor fault types are usually addressed as single sensor faults, occurring in individual sensors. However, as mentioned previously, sensors in real-world SHM systems may experience composite sensor faults, an example of which, consisting of drift and an outlier, is illustrated in Figure 1. As a result, full fault identification needs to address both *single sensor faults* and *composite sensor faults*. The description of the ICSF approach, including two phases, each comprising several steps, are presented in the following section.

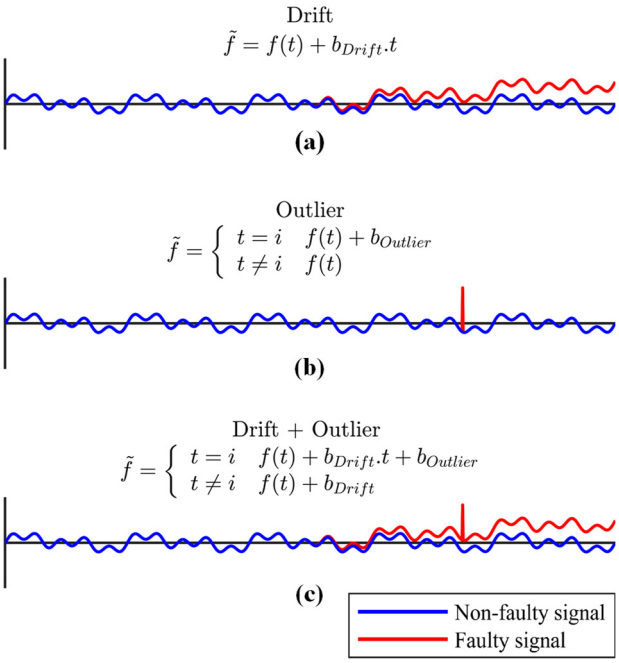

Figure 1: Illustration of a composite sensor fault: (a) a single sensor fault with drift, (b) a single sensor fault with an outlier, and (c) a composite sensor fault consisting of drift and an outlier

Description of the ICSF approach

In this section, the ICSF approach is presented, comprising two phases, (i) preparing the training dataset, and (ii) developing the classification models. A flowchart describing the workflow of the ICSF approach is shown in Figure 2.

Phase 1: Preparing the training dataset

1. Sensor data is recorded by SHM systems within the so-called "data collection period". The total number of data points p recorded by each sensor in the data collection period is representative of the normal operation of the structure.
2. A correlation analysis is conducted on the sensor data to unveil the number of correlated sensors k within a SHM system. Each sensor in the set of correlated sensors is denoted with i (i = 1, …, k). Data recorded by all correlated sensors $f_{1\to k}$ is stored in matrix **A**. As result, matrix **A** has a length equal to the number of data points p, and a width equal to the number of correlated sensors k, as shown in Equation 1.

$$\mathbf{A}_{p\times k} = \begin{bmatrix} f_{1,1} & f_{1,2} & \cdots & f_{1,k} \\ f_{2,1} & f_{2,2} & \cdots & f_{2,k} \\ \vdots & \vdots & \ddots & \vdots \\ f_{p,1} & f_{p,2} & \cdots & f_{p,k} \end{bmatrix} \quad (1)$$

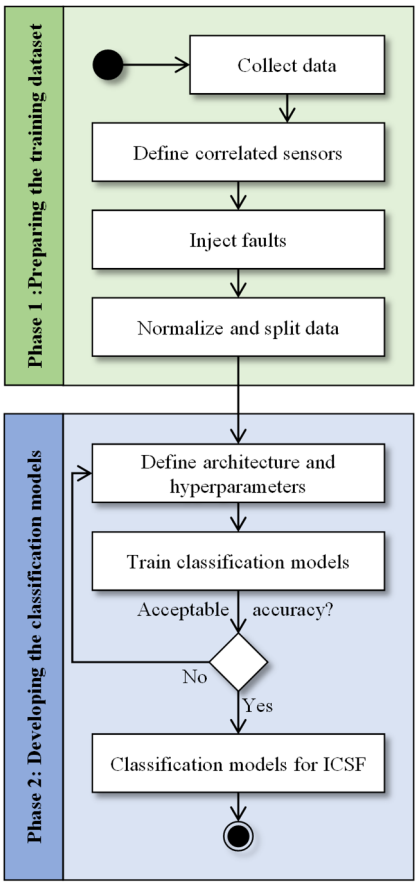

Figure 2: Flowchart of the ICSF approach

3. A total of k input and output datasets are created to train classification models in a later step. The sensor data in matrix **A** are copied into input dataset i (i = 1, …, k), and composite sensor faults are artificially injected into the vector $\mathbf{f}_i$, i.e. in sensor data recorded by sensor i. Injected sensor fault types are stored in the classification output dataset i. As a result, the input dataset i contains clean data from sensors (1, 2, …, i–1, i+1, …k), and sensor data from sensor i with composite sensor faults.
4. Data in the input dataset i is normalized using a minimum-maximum normalization method, shown in Equation 2, to avoid overfitting issues while training the classification models. Then, the normalized input dataset i, as well as the output dataset i are split into training dataset (70%), validation dataset (15%), and testing dataset (15%). In Equation 2, x represents an arbitrary measurement in the sensor data, while x_{min} and x_{max} denote the minimum and maximum measurements in the sensor data, respectively. The variable $x_{normalized}$ corresponds to the normalized value. Both normalization parameters x_{min} and x_{max} used for the input dataset i are saved to be applied to new sensor data that is fed to the classification model M_i after training.

$$x_{normalized} = \frac{x - x_{min}}{x_{max} - x_{min}} \quad (2)$$

Phase 2: Developing the classification models

1. The initial architecture of the LSTM classification network is defined. The LSTM classification network has an input layer, hidden layers, and an output layer. In Figure 3, the general architecture of the LSTM classification network is illustrated. The input layer is a sequence input layer with a length equal to the number of correlated sensors k. The hidden layers include successions of LSTM layers and "dropout" layers. In each LSTM layer, memory cells and a set of gates regulate the flow of data. This architecture enables LSTM layers to capture and retain long-term dependencies in sequential data, making them particularly effective for tasks such as sensor data analysis. In each dropout layer, a probability of dropout is defined representing the likelihood (set between 0 and 1) of randomly neglecting measurements passed through the LSTM layer as means of preventing overfitting. The number of LSTM layers as well as the number of dropout layers may vary based on the model accuracy, which is determined in a later step. The output layers contain a fully-connected layer, a Softmax layer, and a classification layer. The fully-connected layer connects every neuron of the last hidden layer to the neurons of the output layer, representing the number of classes in the classification problem. The Softmax layer is used

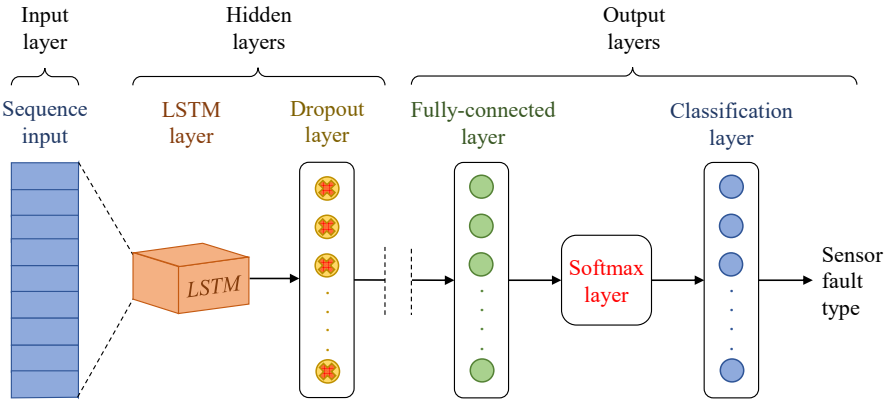

Figure 3: General architecture of the LSTM classification network

between the fully connected layer and the classification layer to convert raw logits into probability distributions, facilitating interpretability, backpropagation, and optimal training. Finally, the classification layer contains all classes of the classification problem, more specifically, the number of sensor fault types c to be included in the FI step. The number of sensor faults c, is calculated using Equation 3, and depends on: (i) the number of single sensor faults m included in each composite sensor fault, and (ii) the total number of single sensor faults n included in all composite sensor faults.

$$c\,(n,m) = \frac{n!}{m!(n-m)} \quad (3)$$

2. One classification model M_i for each correlated sensor i (i = 1, ..., k) is created by training an LSTM using the training dataset i. During training, the training dataset i is fed sequentially (in "batches") to the LSTM classification network, i.e. each batch of the normalized input dataset is fed to the input layer and the corresponding classes of the output dataset are fed to the output layer. The training consists of updating weighted connections between neurons, until the probabilities of the Softmax layer reach a predefined level of accuracy. Thereupon, the classification model M_i is created, capable of recognizing patterns and features in the input dataset i and classifying the sensor data into the corresponding composite sensor fault type. The validation dataset is used to fine-tune the hyperparameters, and prevent overfitting during training.
3. Upon completing training and validating, the accuracy of model M_i is obtained using the testing dataset. For model M_i to be accepted, the classification accuracy must lie above a FI threshold γ. The FI threshold γ is derived following the same rationale as the fault detection threshold γ in previous related research (Al-Zuriqat et al., 2023). Equation 4 introduces the formula to calculate the accuracy (Acc) of the classification model M_i.

$$Acc = \frac{Number\ of\ correct\ preditions}{Total\ number\ of\ preditions} \quad (4)$$

4. Finally, if the accuracy of model M_i is satisfactory, the model is saved to identify faults of sensor i (i = 1, …, k). However, if the accuracy of model M_i is not satisfactory, a different architecture of the LSTM classification network is defined and a new model M_i is trained (back to step 1 of phase 2).

The implementation and validation of the ICSF approach using sensor data from a real-world SHM system installed on a pedestrian bridge is presented in the next section.

Implementation and validation of the ICSF approach

This section describes the implementation and validation of the ICSF approach. To implement the ICSF approach, the programming language MATLAB is utilized to analyze the sensor data, inject faults, and train the classification models. The validation test is carried out using sensor data (acceleration measurements) from a real-world SHM system installed on a pedestrian bridge. First, the pedestrian bridge and the SHM system are presented. Then, the ICSF approach is applied using the acceleration measurements recorded by the real-world SHM system.

Description of the pedestrian bridge and the SHM system

The pedestrian bridge, located in Evosmos, Thessaloniki, Greece, has been a subject of research since the construction in 2016. (Dragos et al., 2020; Smarsly et al., 2022a; and Smarsly et al., 2022b). The pedestrian bridge, is a composite concrete-steel structure, in which a steel structure supports a reinforced-concrete deck. The dimensions of the reinforced-concrete deck are 35.00 m (length) and 4.60 m (width).

Figure 4 illustrates the top view of the pedestrian bridge and the locations of the accelerometers used in the validation test. The SHM system comprises four accelerometers (i.e. S_1, S_2, S_3, and S_4), which have been previously tested and found to be free of faults. The accelerometers are equally distributed along the central axis spanning the length of the bridge, spaced seven meters apart from each other.

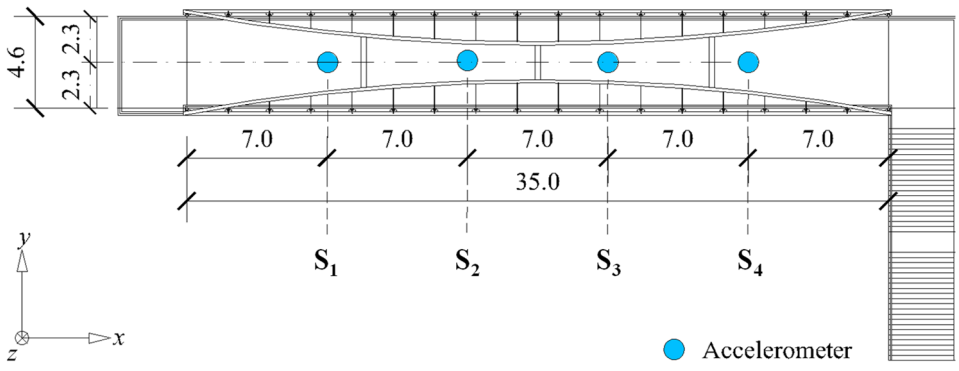

Figure 4: Top view of the pedestrian bridge with the locations of the accelerometers

Description of the validation test

For preparing the training dataset (phase 1), acceleration measurements are recorded by the four accelerometers (S_1, S_2, S_3, and S_4) over data collection period of 90 minutes at a sampling rate of 128 Hz. The total number of data points $p = 692{,}628$ is recorded by each accelerometer.

Next, correlations within the acceleration measurements are investigated via a correlation analysis. A strong correlation has been exposed by the Pearson correlation coefficient among all four accelerometers, i.e. $k = 4$. Notably, the lowest correlation coefficient 0.937 has been observed between sensors S_1 and S_4. Then, the acceleration measurements, recorded by all four correlated accelerometers $f_{1 \to k\,=\,4}$, are stored in matrix $\mathbf{A}_{692628\times4}$.

To determine the sensor fault types to be included in the validation test, as well as the size of the classification layer in a later step, a total of five single faults ($n = 5$) are considered, i.e. bias, drift, gain, precision degradation and outliers. Complete failure, either constant with noise), entails sensors essentially ceasing to operate and can, therefore, hardly be combined with other single sensor faults into composite sensor faults. Combinations of two single faults in the same sensor ($m = 2$) are considered, e.g. drift and outlier at the same time within an individual sensor. As a result, using Equation 3, the total number of composite sensor faults is $c\,(n, m) = 10$. Table 1 provides an overview of the composite sensor faults considered in the validation test.

Table 1: Sensor fault types considered in the validation test

No.	Composite sensor fault
1	Bias + Drift
2	Bias + Gain
3	Bias + Precision degradation
4	Bias + Outliers
5	Drift + Gain
6	Drift + Precision degradation
7	Drift + Outliers
8	Gain + Precision degradation
9	Gain + Outliers
10	Precision degradation + Outliers

Acceleration measurements stored in matrix $\mathbf{A}_{692628\times4}$ are copied into four input datasets. Each input dataset is divided equally into 10 subsets, for which each sensor fault type shown in Table 1 is artificially injected. The classes of the composite sensor faults injected into the input dataset $i\,(i = 1, \ldots, 4)$ is stored in the output dataset $i\,(i = 1, \ldots, 4)$.

Next, acceleration measurements, stored in the input dataset i, are normalized using the minimum-maximum normalization method shown in Equation 2. The normalized input dataset i is split into 70 % training dataset (484,838 data points), 15 % validation dataset (103,894 data points), and 15 % testing data (103,894 data points). Both normalization parameters x_{min} and x_{max} used for the input dataset i during training are saved, to be applied to new sensor data that is fed to the classification model M_i after training.

The initial architecture for the LSTM classification network is defined, with the input layer consisting in a sequence input layer with length $k = 4$. The output layer consists of a fully-connected layer, a Softmax layer, and a classification layer with 10 classes, where each class present a composite sensor fault from Table 1. Three hidden layers are defined, each comprising a LSTM layer followed by a dropout layer. To avoid overfitting during training, the probability of all dropout layers has been set to 20 %.

A total of four classification models, equal to the number of the correlated sensors ($k = 4$), are created by training an equal number of LSTM classification networks. Each model M_i classifies sensor fault types of sensor i, using acceleration measurements from the four correlated sensors of the SHM system as input data. A total training time of 69 minutes for each LSTM classification model is recorded.

Based on Equation 4, the accuracy of the models is evaluated using the testing dataset (103,894 data points). Using a FI threshold $\gamma = 0.85$, a model with an accuracy above 85 % is considered acceptable (Al-Zuriqat et al., 2023). The lowest model accuracy has been observed in model M_2, with an accuracy of 90.3 %.

Finally, the fourth step involves saving all trained classification models M_1, M_2, M_3, and M_4 to identify sensor fault types for sensor S_1, S_2, S_3, and S_4, respectively. The trained classification models are tested using acceleration measurements newly recorded by the SHM system, as presented and discussed in the following section.

Results and discussion

This section presents and discusses the results of applying the classification models (M_1, M_2, M_3, and M_4), obtained by the ICSF approach, to newly recorded acceleration measurements. The acceleration measurements used in the validation test have been recorded by the real-world SHM system and correspond to a data collection period of 30 minutes with a sampling rate of 128 Hz. The total number of data points recorded by each of the accelerometers is $p = 230{,}876$ data points. Subsequently, all composite sensor faults introduced in Table 1 have been randomly injected into the newly recorded acceleration measurements. Table 2 presents the results of

testing the classification models. To determine the accuracy of the classification models, the number of sensor faults identified is compared to the number of sensor faults injected in the testing dataset.

Table 2: Fault identification results of artificially injected sensor fault types including composite faults

Fault type	Sensor	Injected faults	Correctly identified faults	*Acc*
Bias + Drift	S_4	13,607	13,600	99.9 %
Bias + Gain	S_1	13,522	13,411	99.1 %
Bias + Precision degradation	S_2	13,720	13,632	99.3 %
Bias + Outliers	S_3	5,378	4692	87.2 %
Drift + Gain	S_4	13,627	12859	94.3 %
Drift + Precision degradation	S_1	13,390	12,944	96.6 %
Drift + Outliers	S_2	5,461	261	4.7 %
Gain + Precision degradation	S_3	13,638	13,373	98.0 %
Gain + Outliers	S_4	5,556	4,871	87.6 %
Precision degradation + Outliers	S_1	5,398	4,126	76.4 %
Total	**-**	**103,297**	**93,769**	**90.7 %**

As presented in Table 2, the FI capabilities of models M_1, M_2, M_3, and M_4 have been demonstrated using the newly recorded acceleration measurements with artificially injected faults. Out of 103,279 faults injected into the newly recorded acceleration measurements, 93,769 sensor fault types have been correctly identified, representing a total accuracy rate of 90.7 %.

Upon delving deeper into the results of the identification of composite sensor faults, it is noticeable that the classification model achieved the highest accuracy in identifying the composite sensor fault "Bias + Drift" with an accuracy rate of 99.9%. Conversely, a considerably low accuracy rate was observed in the identification of the composite sensor fault "Drift + Outliers" at 4.8%. The low accuracy of identifying the composite fault type "Drift + Outliers" may be attributed to the subtle patterns of outliers, as they correspond to point singularities in a continuous signal, which may be hard to be identified as features by the LSTM classification network.

Summary and conclusions

Fault diagnosis using analytical redundancy, building on mathematical models, has been gaining increasing interest in SHM, owing to the low cost when avoiding redundant sensors, as compared to traditional physical redundancy approaches. Fault diagnosis encompasses fault detection, isolation, identification, and accommodation. Despite the importance of FI in gaining insights into underlying causes of sensor faults within SHM systems, current FI approaches often fail to account for composite sensor faults, which may manifest in real-world SHM systems.

This paper has presented an approach towards identification of composite sensor faults (ICSF). Sensor data with artificially injected composite sensor faults has been used to train LSTM classification networks, addressing composite sensor faults. The ICSF approach has been implemented using the programing language MATLAB, and validated using acceleration measurements recorded by a real-world SHM system. From the results, it is concluded that the ISCF approach has been proven capable of identifying composite sensor faults, thus enhancing the reliability and accuracy of fault diagnosis in SHM systems.

Future work may involve coupling the ICSF approach with other existing fault detection, isolation, and accommodation approaches to establish a comprehensive fault diagnosis concept. Furthermore, the ICSF approach may be embedded into wireless sensor nodes to identify sensor faults on board the sensor nodes within decentralized SHM systems.

Acknowledgments

This paper is the result of a collaborative effort of authors funded by different sources. The authors would like to gratefully acknowledge the support offered by the German Research Foundation (DFG) under grants SM 281/17-1 and SM 281/20-1 as well as by the German Federal Ministry for Digital and Transport (BMDV) within the mFUND program under grant 19FS2013B. Any opinions, findings, conclusions, or recommendations expressed in this paper are those of the authors and do not necessarily reflect the views of DFG or BMDV.

References

Al-Zuriqat, T., Chillón Geck, C., Dragos, K., & Smarsly, K. (2023). Adaptive fault diagnosis for simultaneous sensor faults in structural health monitoring systems. Infrastructures, 8(3), 39.

Cawley, P. (2018). Structural health monitoring: Closing the gap between research and industrial deployment. Structural health monitoring, 17(5), pp. 1225-1244.

Dragos, K. & Smarsly, K. (2016). Distributed adaptive diagnosis of sensor faults using structural response data. Smart Materials and Structures, 25(10), 105019.

Dragos, K., Makarios, T., Karetsu, I., Manolis, G. D., & Smarsly, K. (2020). Detection and correction of synchronization-induced errors in operational modal analysis. Archive of Applied Mechanics, 90(7), pp. 1547-1567.

Frank, P. M. (1990). Fault diagnosis in dynamic systems using analytical and knowledge-based redundancy: A survey and some new results. Automatica, 26(3), pp. 459-474.

Fritz, H., Peralta Abadía, J. J., Legatiuk, D., Steiner, M., Dragos, K., & Smarsly, K. (2022). Fault Diagnosis in Structural Health Monitoring Systems Using Signal Processing and Machine Learning Techniques. Structural Health Monitoring Based on Data Science Techniques, Cury, A., Ribeiro, D., Ubertini, F. & Todd, M. D., Eds. Cham: Springer International Publishing, pp. 143-164.

Isermann, R. & Balle, P. (1997). Trends in the application of model-based fault detection and diagnosis of technical processes. Control engineering practice, 5(5), pp. 709-719.

Kullaa, J. (2013). Detection, identification, and quantification of sensor fault in a sensor network. Mechanical Systems and Signal Processing, 40(1), pp. 208-221.

Kramer, M. A. (1992). Autoassociative neural networks. Computers & chemical engineering, 16(4), pp. 313-328.

Law, K. H., Smarsly, K., & Wang, Y. (2014). Sensor data management technologies for infrastructure asset management. Sensor Technologies for Civil Infrastructures. Wang, M. L., Lynch, J. P. & Sohn, H. Eds. Woodhead Publishing, pp. 3-32.

Li, L., Liu, G., Zhang, L., & Li, Q. (2019). Sensor fault detection with generalized likelihood ratio and correlation coefficient for bridge SHM. Journal of Sound and Vibration, 442(2019), pp. 445-458.

Li, L., Luo, H., Qi, H., & Wang, F. (2023). Sensor Fault Diagnosis Method of Bridge Monitoring System Based on FS-LSTM. Advances in Frontier Research on Engineering Structures, Yang Y., Eds. Singapore: Springer Nature Singapore. pp. 487-501.

Liu, B., Xu, Q., Chen, J., Li, J., & Wang, M. (2022). A New Framework for Isolating Sensor Failures and Structural Damage in Noisy Environments Based on Stacked Gated Recurrent Unit Neural Networks. Buildings, 12(8), 1286.

Patton, R. J. (1990). Fault detection and diagnosis in aerospace systems using analytical redundancy. In: IEE Colloquium on Condition Monitoring and Fault Tolerance. London, UK, 11/06/1990.

Rao, A. R. M., Kasireddy, V., Gopalakrishnan, N., & Lakshmi, K. (2015). Sensor fault detection in structural health monitoring using null subspace–based approach. Journal of Intelligent Material Systems and Structures, 26(2), pp. 172-185.

Smarsly, K. & Petryna, Y. (2014). A Decentralized Approach towards Autonomous Fault Detection in Wireless Structural Health Monitoring Systems. In: Proceedings of the 7th European Workshop on Structural Health Monitoring (EWSHM). Nantes, France, 07/08/2014.

Smarsly, K. & Law, K. H. (2014). Decentralized Fault Detection and Isolation in Wireless Structural Health Monitoring Systems using Analytical Redundancy. Advances in Engineering Software, 73(2014), pp. 1-10.

Smarsly, K., Dragos, K., & Kölzer, T. (2022a). Sensor-integrated digital twins for wireless structural health monitoring of civil infrastructure [Sensorintegrierte digitale Zwillinge für das automatisierte Monitoring von Infrastrukturbauwerken]. Bautechnik 99(6), pp. 471-476.

Smarsly, K., Worm, M., & Dragos, K. (2022b). Design and validation of a mobile structural health monitoring system based on legged robots. In: Proceedings of the 29th International Workshop on Intelligent Computing in Engineering (EG-ICE). Aarhus, Denmark, 07/08/2022.

Steiner, M., Legatiuk, D. & Smarsly, K. (2019). A support vector regression-based approach towards decentralized fault diagnosis in wireless structural health monitoring systems. In: Proceedings of the 12th International Workshop on Structural Health Monitoring (IWSHM). Stanford, CA, USA, 09/10/2019.

Yan, K., Zhang, Y., Yan, Y., Xu, C., & Zhang, S. (2020). Fault diagnosis method of sensors in building structural health monitoring system based on communication load optimization. Computer Communications, 159(2020), pp. 310-316.

Yu, C. B., Hu, J. J., Li, R., Deng, S. H., & Yang, R. M. (2014). Node fault diagnosis in WSN based on RS and SVM. In: 2014 International Conference on Wireless Communication and Sensor Network (IEEE). Wuhan, China, 12/14/2014.

Zhang, Z., Mehmood, A., Shu, L., Huo, Z., Zhang, Y., & Mukherjee, M. (2018). A survey on fault diagnosis in wireless sensor networks. IEEE Access, 6(2018), pp. 11349-11364.